Materials Science and Engineering C xxx (2010) xxx–xxx

Contents lists available at ScienceDirect

Materials Science and Engineering C

journal homepage: www.elsevier.com/locate/msec

Structural characterization and mechanical behavior of a bivalve shell (*Saxidomus purpuratus*)

Wen Yang [a,b], Neima Kashani [c], Xiao-Wu Li [a], Guang-Ping Zhang [b], Marc André Meyers [c,*]

[a] Institute of Materials Physics and Chemistry, College of Sciences, Northeastern University Shenyang 110004, PR China
[b] Shenyang National Laboratory for Materials Science, Institute of Metal Research, Chinese Academy of Sciences, 72 Wenhua Road, Shenyang 110016, PR China
[c] Department of Mechanical and Aerospace Engineering, Materials Science and Engineering Program, University of California, San Diego, La Jolla, CA 92093-0411, USA

ARTICLE INFO

Article history:
Received 20 March 2010
Received in revised form 24 September 2010
Accepted 10 October 2010
Available online xxxx

Keywords:
Biological
X-ray diffraction
Structure
Hardness
Compression
Shells

ABSTRACT

The structure and mechanical behavior of *Saxidomus purpuratus* bivalve shell were investigated. XRD results show that the only form of calcium carbonate present in the shell is aragonite. The inner and middle layers have a cross-lamellar structure, while the outer layer has porosity and does not have tiles, but instead has 'blocky' regions. The hardness of middle and inner layer are close in both plane view and cross section, but the hardness of outer layer is significantly less, especially in the plane view. The compressive strengths with loading along the three orientations were established and significant differences were found. The Weibull strength at 50% of the probability of failure varies between 59 and 148 MPa and is dependent on the loading orientation and in condition of shell (dry vs. hydrated). These differences are interpreted in terms of the anisotropic structure and coarser structure of the external layer.

1. Introduction

Through natural selection over hundreds of millions of years, mollusk shells have developed their structure and mechanical properties to protect themselves from attack by a variety of marine predators, which try to break it using compressive force application, prying attack or nipping attempt. Hence, their properties, considering the simple constituents, are much better than man-made materials. The components of biological shells are calcium carbonate which is in general about 95 wt.% and less than 5 wt.% organic materials [1–3]. The two principal polymorphs of calcium carbonate in shells are aragonite and calcite. X-ray diffraction (XRD) is usually used to detect the detailed structure of these minerals. In 1960, Lutts et al. [4] identified the calcium carbonate phases for 19 mollusk shells. In 1963, Wilbur and Watabe [5] studied the regeneration process with some mollusk species and found that the crystalline phase in some species was not changed during regeneration. Calcium carbonate changed from the amorphous state to aragonite during the growth of the shells. Calcite traces were only detected in some organisms [6]. Investigators analyzed the $CaCO_3$ polymorphs in different kinds of shells with different treatments [7–15]. Most of the shells contain aragonite. Some species have both aragonite and calcite, such as *Pecten maximus*, that contains aragonite and calcite in a proportion of 3:7. The external layer in abalone is also calcitic. Paula and Silveira [16] summarized the analytical methods including XRD method. The different $CaCO_3$ polymorphs can form different types of morphologies, such as prismatic structure, sheet nacreous structure, lenticular nacreous structure, foliated structure, cross-lamellar structure, complex cross-lamellar structure and homogeneous structure [17,18].

These structures, with simple components, can result in outstanding properties, such as flexure strength and toughness. The compression strengths of a significant number of shell species have already

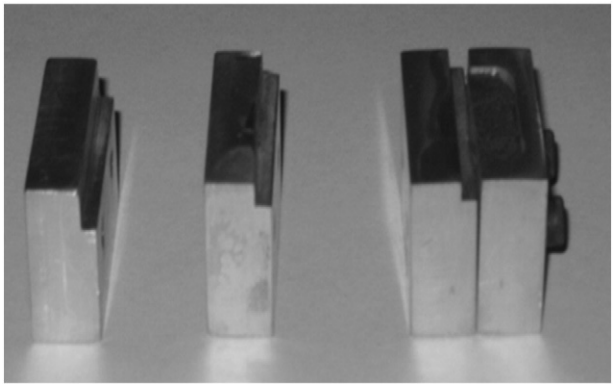

Fig. 1. Fixture used to prepare the specimens. Left and middle: separate components for different sizes. Right: assembled fixture.

* Corresponding author. Tel.: +1 858 534 4719; fax: +1 858 534 5698.
E-mail address: mameyers@ucsd.edu (M.A. Meyers).

0928-4931/$ – see front matter © 2010 Elsevier B.V. All rights reserved.
doi:10.1016/j.msec.2010.10.003

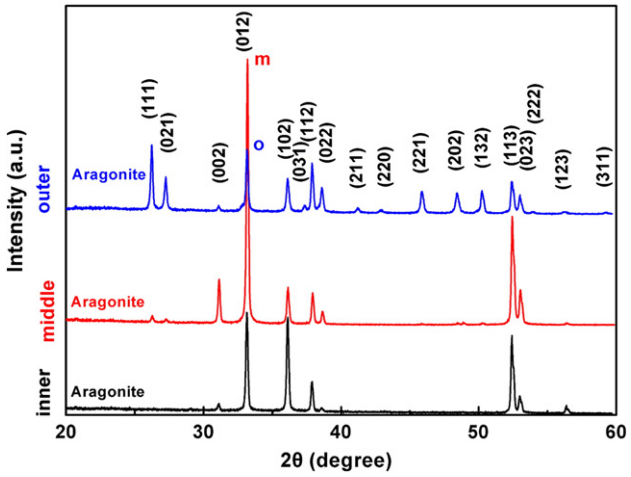

Fig. 2. XRD results of inner (bottom), middle and outer (top) layers of *Saxidomus purpuratus* shell. All the layers are aragonite. Outer layer has more peaks than inner and middle layers.

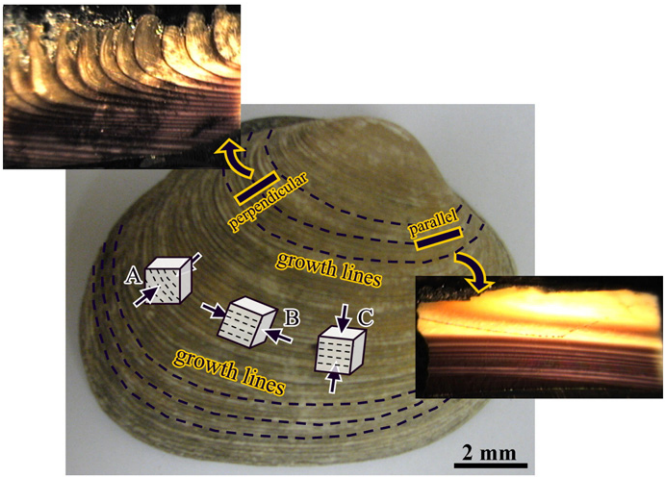

Fig. 3. Cross sections parallel and perpendicular to growth lines of *Saxidomus purpuratus* shell and the orientations of compression specimens: Orientation A, loading perpendicular to the shell surface; Orientation B, loading parallel to the shell surface and growth lines; Orientation C, loading parallel to the shell surface and perpendicular to the growth lines.

been investigated [1,17–25]. The high strength and good toughness of shells were first identified by Currey and Taylor [1,18–20]. They attested that the strongest shells had nearly twice the compressive strength of bone. Although the flexure strength of shells with some structures, such as homogeneous structure, is not as high as that of bone, the compression strengths of shells can be much higher than bone [17]. Bone has a compression strength of between 88 and 232 MPa and a tension strength between 80 and 138 MPa[17,26].

Menig et al. [21,22] investigated the quasi-static and dynamic mechanical response of *Haliotis rufescens* and *Strombus gigas* including compression and analyzed the results by Weibull statistics. They showed that the quasi-static compression strength (measured as failure probability of 50% [P(V) = 0.5]) of abalone and conch are 540 MPa and 166 MPa respectively for loading perpendicular to the shell surfaces; and 235 MPa and 310 MPa respectively for loading parallel to the shell surfaces. Lin et al. [23] later investigated the mechanical properties of a clam called *Tridacna gigas* and compared the results with those obtained by Menig et al. [21,22]. They found that the compression strength of red abalone (*Haliotis rufescens*) is about twice as that of clam (*Tridacna gigas*) and four times as that of conch (*Strombus gigas*). This difference is the direct consequence of the much lower fraction of the mineral component in bone: approximately 0.3 to 0.6 on a volume basis.

Herein, the structure of *Saxidomus purpuratus* shells was characterized by X-ray diffraction and scanning electron microscopy (SEM), and some mechanical properties including hardness and compression behavior were investigated.

Table 1
Calcium carbonate polymorphs of different shells with different state and treatments. (A: aragonite, C: calcite).

	Organisms	State tested	Treatment	Mineral	Ref
Gastropoda	*Haliotis rufescens*	Powder	R.T.	A	13,14
		Powder	500 °C, 10 min	A→C	14
	Stromubus gigas	Bulk/ powder		A	8,9,11
	Pomacea canaliculata Lamarck	Powder	Unannealed	A	12
			Annealed, >400 °C	A→C	12
			Annealed, 500 °C	C	12
			Annealed, 900 °C	CaO	12
	Trochus maculates	Powder		A	13
	"Flat pearl" (nacreous, block-like, spherulitic layer)	Plane view		A	7
	"Flat pearl" (prismatic layer)	Plane view		C	7
Bivalve	*Tridacna gigas*	Bulk		A	9
	Meretrix lusoria	Powder/ bulk		A	10, 13
	Preria penguin	Powder/ bulk		A	10, 13
	Pecten maximus	Powder		A(30%) + C	13
	Tellinella asperrima	Powder/ nacre		A	15
	Saxidomus purpuratus	Inner/ middle/ outer layers		A	Present work

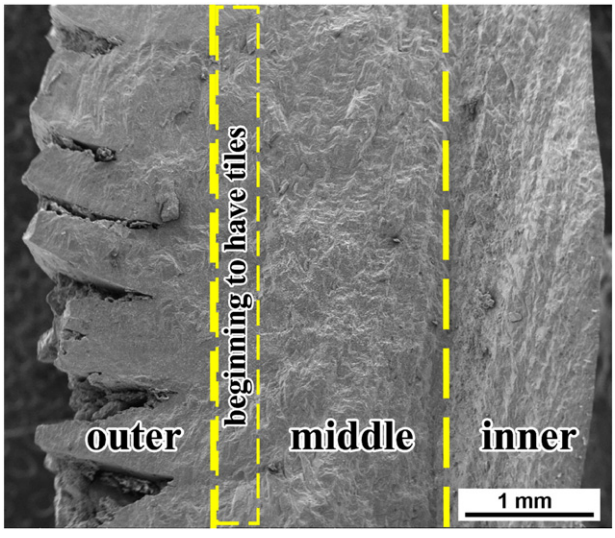

Fig. 4. Overall view of the cross section perpendicular to the growth lines.

2. Experimental techniques

The *Saxidomus purpuratus* shells, which are bivalves and like to live in groups in the water rich with diatom foods, were collected from Bo/Huang Sea Area near Dalian city in China. This kind of shell was chosen because its thickness is sufficient so that the specimens can be prepared in different orientations. They were cleaned carefully and dried in air at room temperature. Specimens were cut with a water-cooled low-speed diamond saw. The specimens used in XRD test, OM observation and hardness testing were ground with sand paper from 400# to 2000# and polished carefully to decrease the size and the number of the microcracks.

Plane view specimens of inner, middle and outer layers with a length of about 1.2 mm were prepared to perform XRD test using Rigaku MiniFlex II Desktop X-ray Diffractometer with Cu K_α radiation. The inner and outer layer specimens were polished from inner and outer layer, respectively, until they were just flat, and the middle layer specimen was chosen approximately in the middle of the thickness of the shell. The structures of shells were observed with a FEI scanning electron microscope of the fractured specimens along planes parallel and perpendicular to the surface markings indicating growth lines after being gold sputtered. Hardness tests were carried out with plane view specimens of the three layers and cross section specimens, parallel and perpendicular to the growth lines using loads of 100 gf

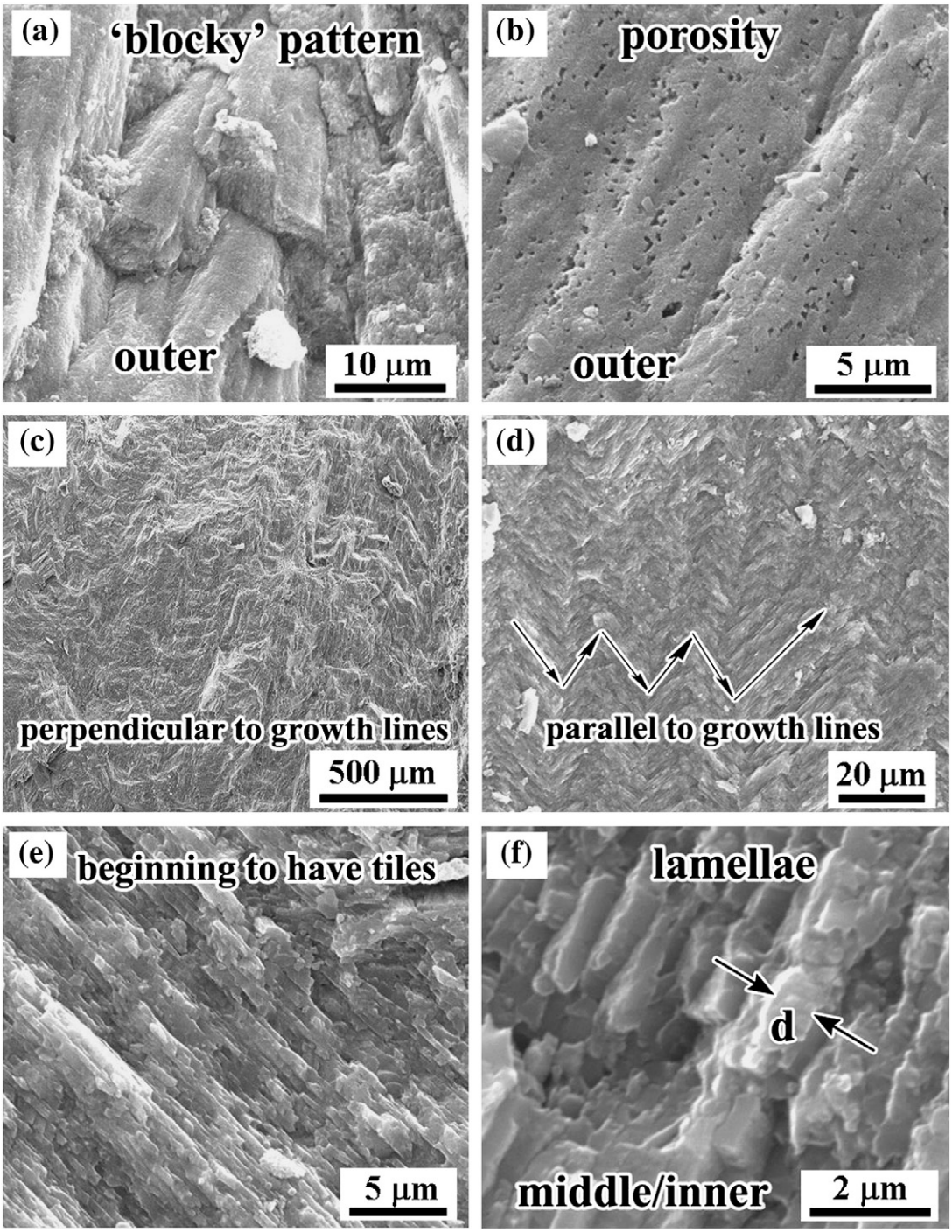

Fig. 5. Structural characterizations of the shell. (a) Blocky pattern of outer layer, (b) outer layer with porosity, (c) cross section perpendicular to growth lines, (d) cross section parallel to growth lines, (e) region close to outer layer beginning to have tiles in the middle layer, and (f) the lamellae in middle and inner layers.

Please cite this article as: W. Yang, et al., Materials Science and Engineering C (2010), doi:10.1016/j.msec.2010.10.003

and 200 gf with a Leco M-400-H1 hardness testing machine. The indentations were separated sufficiently to ensure that the indentation regions would not affect the adjacent regions. Dry and wet compression specimens with approximate dimensions of $3.5 \times 3.5 \times 3.5$ mm were prepared in three orientations: loading perpendicular to the shell surface (A), parallel to the shell surface and growth lines (B) and parallel to the shell surface but perpendicular to the growth lines (C).

Wet (hydrated) compression specimens were prepared with a special fixture to ensure that the two surfaces of the specimens loaded were flat and parallel (Fig. 1). The shells for these tests were about 3–8 mm thick. This thickness allowed the samples to be polished until their edges where parallel, eliminating the irregularities and non-parallelism in their surfaces. The diamond blade cuts were made without removing the specimen from the grips to ensure parallelism of the surfaces being tested. A thin sheet of plastic and grease were used to minimize stress concentrations of the contact regions with the platens. All the compression specimens were tested under constant loading rate of 1×10^{-3} s^{-1} in an Instron 3367 testing machine.

3. Results and discussion

3.1. Structural characterization

Fig. 2 shows the XRD patterns obtained from the inner, middle and outer layers of the shells. The intensity and *d* spacings of the labeled peaks of the three layers correspond to the 2θ angles of XRD peaks of aragonite. The inner layer shows a distinct texture. The intensities of the (012), (102) and (113) reflections are much stronger than other reflections. The middle layer shows a similar peak intensity distribution as the inner layer, but its (102) peak is not as strong as that of inner layer. However, the outer layer shows more XRD peaks than the others. As most of the mollusk shells, the main $CaCO_3$ configuration existing in the shell is aragonite. Table 1 shows calcium carbonate polymorphs for different shells. Only a few shells, such as *Pecten maximus* [13], contain both aragonite and calcite. When heated to a temperature of about 400 °C or 500 °C, the structure of the shells changes from aragonite to calcite. This transformation occurs because aragonite is a thermodynamically unstable phase of calcium carbonate which exists stably with the present of organic compound at room temperature [27].

Fig. 3 shows the cross-sectional morphologies parallel and perpendicular to the growth lines of the shell and the three orientations of the compression specimens with loads. The dashed lines on the little cubes stand for the growth lines. The OM pictures show an alternation of light and dark layers. The light region is the outer layer. The layers in the cross section parallel to the growth lines correspond to the shape of shell in that part. The layers in the cross section perpendicular to the growth lines taken from the edge of shell show an outward curvature. In the edge of the shell, the inner layers are parallel to each other and follow the shape of shell, but when they reach the outer layer, they bend toward the surface of the shell. These layers represent the growth sequence in the shell, as it increases in both size and thickness.

The detailed structure of the shell is seen in Fig. 4 (SEM), which shows the whole view of the cross section perpendicular to the growth lines. The approximate ranges of outer, middle, and inner layers are shown in the picture. Higher magnification was used to distinguish the differences between the structures of three layers. Fig. 5(a) shows the 'blocky' pattern of the outer layer and its detailed porous structure is shown in Fig. 5(b); as one goes toward the middle layer, the structure begins gradually to have tiles. The middle and inner layers have similar crossed-lamellar structure. Fig. 5(c) and (d) shows the morphologies of the cross section perpendicular and parallel to the growth lines, respectively. The orientations of the lamellae are pointed by arrows. Fig. 5(e) shows parallel arrays of tiles (lamellae) in the transition region. Fig. 5(f) shows the lamellae in the middle and inner layer whose average thickness, d, of about 250 nm. The thickness of these tiles (lamellae) is lower than that of the abalone (~450 nm) [21] and of the bivalve Araguaia shell (~1500 nm). [28].

3.2. Mechanical properties

The hardness was measured with five measurements in the plane view and one measurement in the cross sections. This was done to establish whether it changes from outer to inner portions of the shell both parallel and perpendicular to the growth lines. The length of the diagonal of the indentation is about 25–75 μm. The corners of some indentation were damaged or broken. Some cracks spread around from the tip of the indentation, and some weak lamellae are lost in the corner by the load. The hardness is calculated by the equation [29],

$$HV = \frac{2P\sin(\alpha/2)}{d^2} = \frac{1.8544P}{d^2} \quad (1)$$

in which *P* is the applied load (in kgf), *d* is the average length of the diagonals (in mm) and α is the angle between the opposite surfaces of the indenter (136°). The results are shown in Fig. 6(a) and (b), respectively. The horizontal coordinate represents the normalized distance from outer layer to inner layer, and the Y coordinate represents the hardness. The variation in hardness is more distinct under loading of 100 gf. One can see the trend of the hardness in the

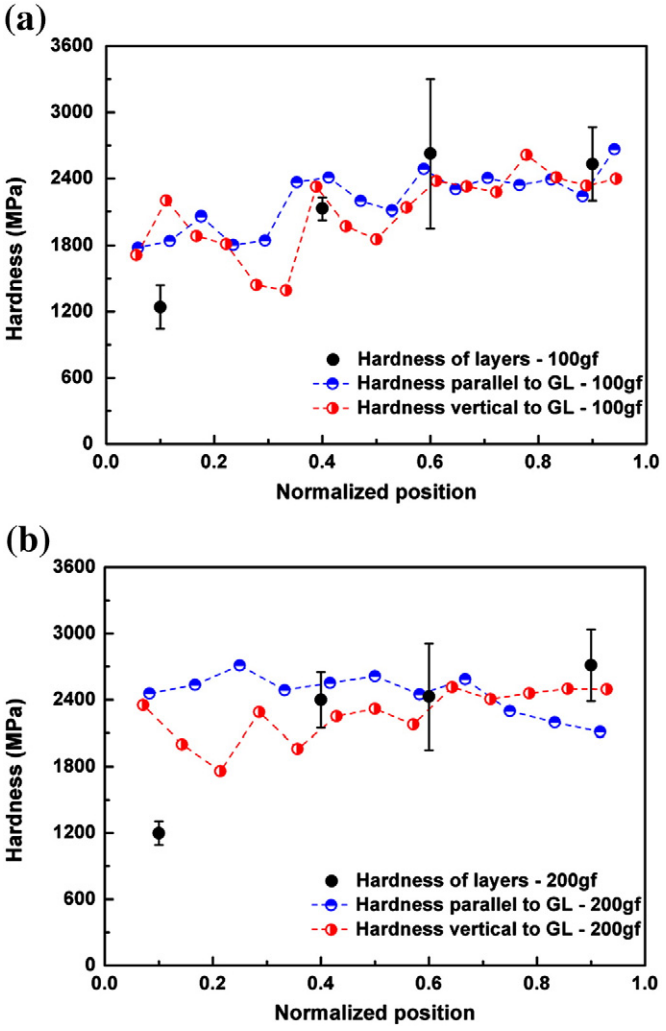

Fig. 6. Hardness across cross sections parallel and perpendicular to the growth lines (GL) as a function of the normalized position (x = 0.0–1.0) from outer to inner layer; loads of (a) 100 gf and (b) 200 gf. Hardness along plane view (taken in the positions).

cross section from the outer layer to inner layer in Fig. 6(a). Among the three layers in the cross section, the hardness of outer layer is lowest but varies greatly. The hardness of cross section perpendicular to the growth lines varies more than that of cross section parallel to the growth lines. The hardness of plane view layers is easier to evaluate under the load of 200 gf, and is shown in Fig. 6(b). The hardness (plane view) of outer layer (~1200 MPa) is considerably lower than those of middle (~2400 MPa) and inner layer (~2700 MPa) due to their different structures and porosities.

The compression strengths were obtained from about 10 specimens in each orientation and analyzed by the Weibull method and are shown in Fig. 7. The specimens in Orientation A are much harder to obtain because the shell was too thin in some areas for a 3.5 mm specimen to be made from it. A typical stress-strain plot tested in Orientation B is shown in Fig. 7(a). The compression strength and modulus are 88.3 MPa and 11.9 GPa, respectively. The two drops in load (marked by arrows) indicate that the cracks that formed were often of the 'axial splitting' kind and the specimens were not damaged catastrophically. Fig. 7(b)–(d) shows the compression strengths fitted with Weibull curves for Orientations A, B and C, respectively. These orientations are defined in Section 2. As seen above, the hardness in Orientation C is the highest, while the hardness in Orientation A is the lowest. The compression strengths obtained with dry/wet specimens (50% of the probability of failure) are 101.6/109.8 MPa and 101.8/148.0 MPa in Orientations B and C, respectively, while the one for Orientation A is lower (58.8/105.0 MPa). The strength in Orientations A and C for dry differ considerably from the strength for wet in the same orientations, respectively. This is well known for shells and has been attributed to the effect of hydration on the mechanical properties of the organic interlayer. The Weibull modulus, which depends on the distribution of flaw sizes [30,31], is a measure of the variability of strength. The higher the value of m, the less the variability of the material strength is [29]. So, there is less variation in the compression strengths in Orientations B (m = 4.81, 2.21) and C (m = 4.42, 3.93) than in Orientation A (m = 2.67, 2.36). This indicates that mechanical properties of the shell are anisotropic. One possible reason for the difference is that the compressive specimens incorporate both the external and internal regions, which have different strengths. When loading is applied perpendicular to the surface, the two components are in series and the strength of the weakest component (the outside layer) determines the strength of the specimen. On the other hand, when loading is applied in the plane of the shell, the two components are in parallel and subjected to the same stress. The strongest (middle and inner layers) can carry load to a higher level than the outside, and the specimens are consequently stronger. The compressive strengths of the Araguaia bivalve shells [28] (the strongest in compression studied by our group) were 567 MPa perpendicular and 347 MPa parallel to surface. Hence, *Saxidomus purpuratus* is also much weaker than the shells previously mentioned, such as abalone and conch [21,22]. This can be attributed

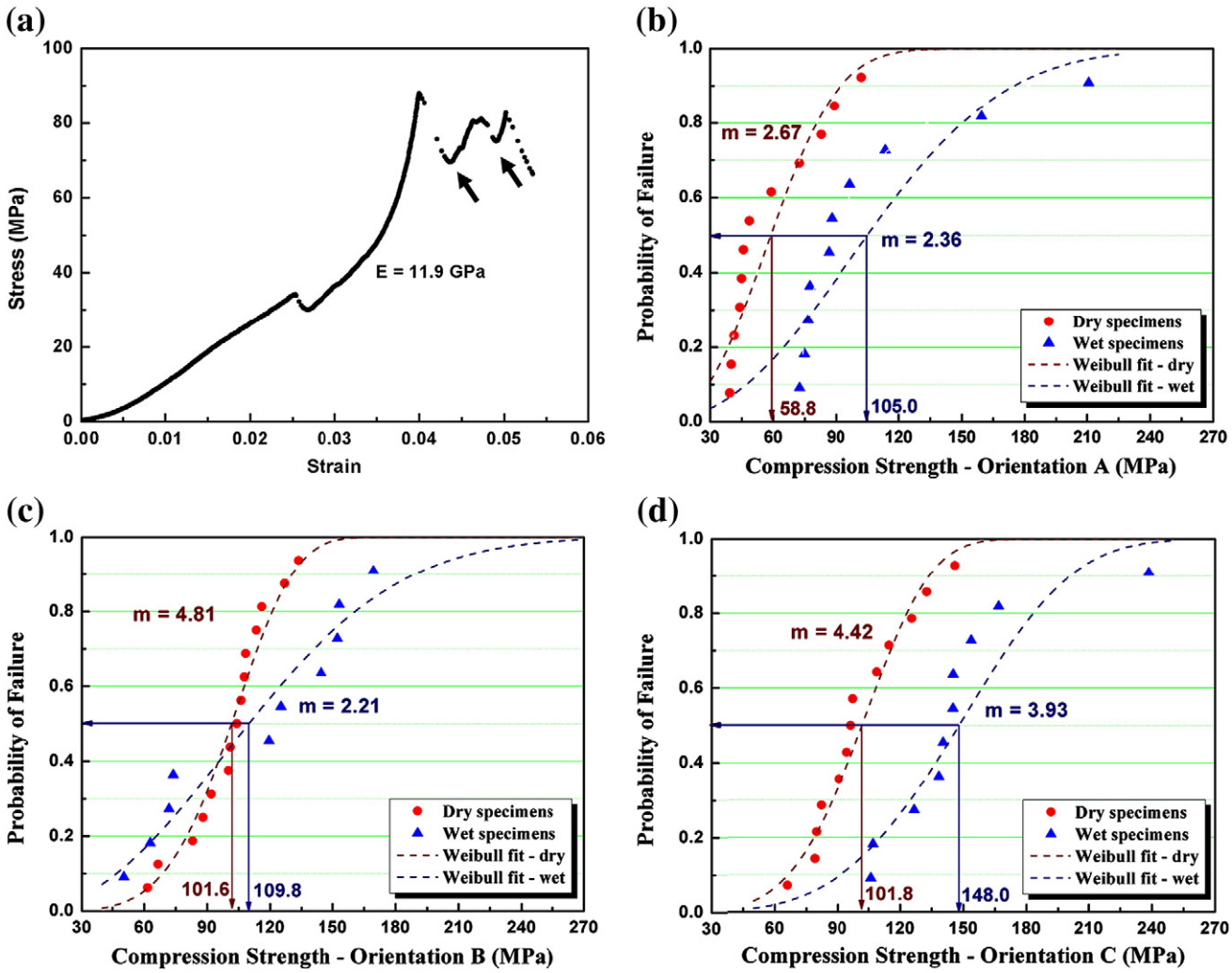

Fig. 7. Compression test results; (a) a typical stress-strain plot obtained in Orientation B; (b) Weibull fit of dry and wet specimens in Orientation A; and (c, d) Weibull fit of dry and wet specimens in Orientations B and C, respectively.

Please cite this article as: W. Yang, et al., Materials Science and Engineering C (2010), doi:10.1016/j.msec.2010.10.003

to a lower fraction of organic material in the structure of the *Saxidomus* shell.

4. Conclusions

The structure of *Saxidomus purpuratus* shells was analyzed by XRD, OM and SEM. The mechanical properties were investigated through hardness and compression tests. The calcium carbonate exists in aragonite structure in the three layers. The outer layer has a porous blocky structure, while the middle and inner layers have a cross-lamellar structure with distinct XRD patterns. The hardness in plane view of the outer layer is much lower than that of the inner and middle layer and varies considerably in the cross sections, both perpendicular and parallel to the growth lines. The hardness of middle and inner layers show less variability than that of the outer layer. The compression strength with loading perpendicular to the surface of the shell is the lowest and shows the greatest variation. Because the component with the lowest strength (outside) fails first and its strength determines the overall strength. For the other two loading directions, the interface is parallel to the loading direction and the two regions act as springs in parallel. The strengths vary between approximately ~50 and 150 MPa, which is much lower than shells previously studied by our group. These ranged from ~160 to ~550 MPa [21–23,28].

Acknowledgements

This work was supported by NSF DMR Biomaterials Program at UCSD. We thank the following persons that have contributed significantly to this work: C.T. Wei, for assisting with mechanical testing and XRD, Y.S. Lin, for assisting with the hardness testing, J. Kiang, for assisting with the compression tests, A. Suwarnasarn, for helping with SEM observation, M.L. Li and Y. Li, for helping with interpretation of the XRD results. P.Y. Chen and I.H. Chen helped with several aspects of the research.

References

[1] J.D. Currey, Proc. R. Soc. Lond. 196 (1977) 443.
[2] K. Okumura, P.G. Gennes, Eur. Phys. J. E 4 (2001) 121.
[3] G. Kramptz, G. Graser, Science 255 (1992) 1098.
[4] A. Lutt, J. Grandjean, Ch. Grégorie, Arch. Int. Physiol. Biochim. 68 (1960) 829.
[5] K.M. Wilbur, N. Watabe, Ann. NY Acad. Sci. 109 (1963) 82.
[6] D. Medakovié, S. Popovié, B. Grzeta, M. Plazonié, M. Hrs-Brenko, Mar. Biol. 129 (1997) 615.
[7] X.W. Su, A.M. Belcher, C.M. Zaremba, D.E. Morse, G..D. Stucky, A.H. Heuer, Chem. Mater. 14 (2002) 3106.
[8] X.W. Su, D.M. Zhang, A.H. Heuer, Chem. Mater. 16 (2004) 581.
[9] X. Zhang, K.S. Vecchio, Mater. Sci. Eng. C 26 (2006) 1445.
[10] Z.H. Zhu, H. Tong, Y.Y. Ren, J.M. Hu, Micron 37 (2006) 35.
[11] K.S. Vecchio, X. Zhang, J.B. Massie, M. Wang, C.W. Kim, Acta Biomater. 3 (2007) 910.
[12] N. Udomkan, P. Limsuwan, Mater. Sci. Eng. C 28 (2008) 316.
[13] F.D. Fleischli, M. Dietiker, C. Borgia, R. Spolenak, Acta Biomater. 4 (2008) 1694.
[14] Z.W. Huang, X.D. Li, Mater. Sci. Eng. C 29 (2009) 1803.
[15] F.Z. Ren, X.D. Wan, Z.H. Ma, J.H. Su, Mater. Chem. Phys. 114 (2009) 367.
[16] S.M. de Paula, M. Silveira, Micron 40 (2009) 669.
[17] J.D. Taylor, M. Layman, Palaeontology 15 (1972) 73.
[18] J.D. Currey, J.D. Taylor, J. Zool. Lond. 173 (1974) 395.
[19] J.D. Currey, J. Zool. 180 (1976) 445.
[20] J.D. Currey, Biorheology 2 (1964) 1.
[21] R. Menig, M.H. Meyers, M.A. Meyers, K.S. Vecchio, Acta Mater. 48 (2000) 2383.
[22] R. Menig, M.H. Meyers, M.A. Meyers, K.S. Vecchio, Mater. Sci. Eng. A 297 (2001) 203.
[23] A.Y.M. Lin, M.A. Meyers, K.S. Vecchio, Mater. Sci. Eng. C 26 (2006) 1380.
[24] R.Z. Wang, Z. Suo, A.G. Evans, N. Yao, I.A. Aksay, J. Mater. Res. 16 (2001) 2485.
[25] F. Barthelat, H. Tang, P.D. Zavattieri, C.M. Li, H.D. Espinosa, J. Mech. Phys. Solids 55 (2007) 306.
[26] J.D. Currey, Clin. Orthop. 73 (1970) 210.
[27] S. Weiner, L. Addadi, Trends Biochem. Sci. 16 (1991) 252.
[28] P.-Y. Chen, A.Y.M. Lin, Y.-S. Lin, Y. Seki, A.G. Stokes, J. Peyras, E.A. Olevsky, M.A. Meyers, J. McKittrick, J. Mech. Behav. Biomed. Mater. 1 (2008) 208.
[29] M.A. Meyers, K.K. Chawla, Mechanical behavior of materials, Prentice-Hall, USA, 1999.
[30] A.D.S. Jayatilaka, K. Trustrum, J. Mater. Sci. 12 (1977) 1426.
[31] R. Danzer, J. Eur. Ceram. Soc. 10 (1992) 461.

Please cite this article as: W. Yang, et al., Materials Science and Engineering C (2010), doi:10.1016/j.msec.2010.10.003